Two-Photon Photoemission as a Probe of Electron Interactions with Atomically Thin Dielectric Films on Metal Surfaces

D. F. Padowitz, W. R. Merry, R. E. Jordan, and C. B. Harris

Department of Chemistry, University of California, Berkeley, California 94720
and Chemical Sciences Division, Lawrence Berkeley Laboratory, Berkeley, California 94720

Electrons bound to a metal surface by the image potential are seen to persist in the presence of various adsorbates. A new two-photon photoemission spectrometer with high resolution and sensitivity permits precise measurement of adsorbate-induced changes in image state binding energy and dispersion. This provides a unique probe of electron interaction with thin dielectric films. Monolayer xenon on Ag(111) reduced the electron's effective mass. Spectra of alkane multilayers show rich structure with layer-by-layer shifts in binding energy. Bilayers gave evidence of electron localization.

We have found that electrons in image-potential states at a metal surface remain observable in the presence of monolayers to multilayers of a number of adsorbed molecules. These electrons, bound a few angstroms outside the metal, are sensitive to the interfacial potentials and interact strongly with the adsorbed molecules. To explore these states we have developed a new instrumental approach to two-photon photoemission spectroscopy with both excellent energy resolution and much greater sensitivity than previous systems. We have initiated a systematic study of adsorbate-induced changes in the binding energies and dispersions of the image-potential states on a metal surface. The results provide a unique view of the electronic properties of interfaces and thin films.

The image potential is an attractive force experienced by a charged particle outside a polarizable surface due to the surface charge redistribution the particle induces. The image potential supports bound states which exist as ordinarily unoccupied electronic levels on both metal and insulator surfaces [1,2]. The image-potential states form a Rydberg-like series of excited states, labeled by a single quantum number n, converging to the vacuum level. On metals the $n = 1$ image state is bound 0.5–0.8 eV below the vacuum level. In the past several years image states on clean metal surfaces have been studied extensively [3–5].

Figure 1 indicates the approximate extent of the wave functions for an electron in the $n = 1$ or $n = 2$ image states of the clean Ag(111) surface, compared to the thickness of an adsorbed Xe monolayer. This picture, based on hydrogenic wave functions, is schematic, but makes it clear that the electron should interact strongly with the adsorbate and be sensitive to potentials at both the metal/adsorbate and adsorbate/vacuum interfaces. Furthermore, the range of interaction will vary with quantum number.

To probe these excited electronic states we use the technique of two-photon photoemission [6]. The first photon promotes an electron from an occupied state to a bound excited state. The second photon then photoemits

the excited electron and the energy of the excited state is determined from the difference in energy between the emitted electron and the second photon. The new instrument developed for this work is based on time-of-flight analysis of the electron's energy using delayed-coincidence counting and a picosecond laser with a megahertz repetition rate. Low energies in each laser pulse eliminate space charge which can degrade energy resolution, while the high repetition rate insures that the signal remains high, typically 10^4 counts/s. Based on the measured timing accuracy and flight distance, and assuming no perturbing fields in the flight region, energy resolution is on the order of 5 meV.

The metal substrate was a single-crystal Ag(111) surface which was sputtered and annealed before each set of experiments. The work function was measured to be 4.55 eV by threshold photoemission. To ensure free flight of the photoelectrons, the contact potential between the sample and detector was offset by an applied bias of a few tenths of a volt. This bias was adjusted to compensate for the work-function change during adsorption. In some cases uncertainties in work function limited the accuracy in determining absolute binding energies to ±0.05 eV. The $n = 1$ image state on the clean metal was bound by 0.78 eV.
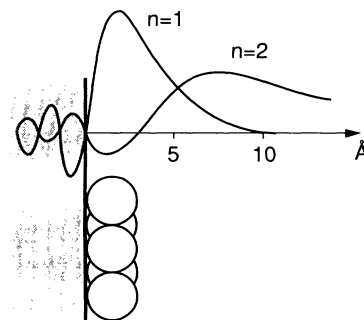

FIG. 1. Approximate wave functions for the first two image-potential states of a clean metal surface compared to the thickness of a xenon monolayer.

An ordered monolayer of Xe was grown on Ag(111) simply by maintaining a surface temperature between 70 and 80 K and a background Xe pressure near 1×10^{-6} Torr [7]. For the Xe-covered surface the work function shifted by -0.45 eV. Figure 2(a) shows the two-photon photoemission spectrum for the $n=1$ state on the Xe-covered surface, biased to zero field, compared to that of the clean surface. These spectra were measured at 75 K, at wavelengths of 285 and 570 nm for the clean surface or 323 and 646 nm for the Xe monolayer. The Xe-covered surface was excited at longer wavelength because of its lowered work function, in order to remain below the single-photon photoemission threshold and insure that the electrons are excited from similar initial states of the metal. Previous experiments using inverse photoemission spectroscopy (IPS) saw that the image state remained approximately pinned to the vacuum level as the work function of the substrate is changed [8]. The present experiments, with energy resolution at least an order of magnitude better than IPS, are sensitive to small changes in the image state binding energy. Nevertheless, within 50 meV, no change in the $n=1$ binding energy was detected for a Xe monolayer.

These results were contrary to our initial expectation that interposing a dielectric layer between the electron and its image in the metal would reduce the binding energy. If the electron were within the adsorbate layer,
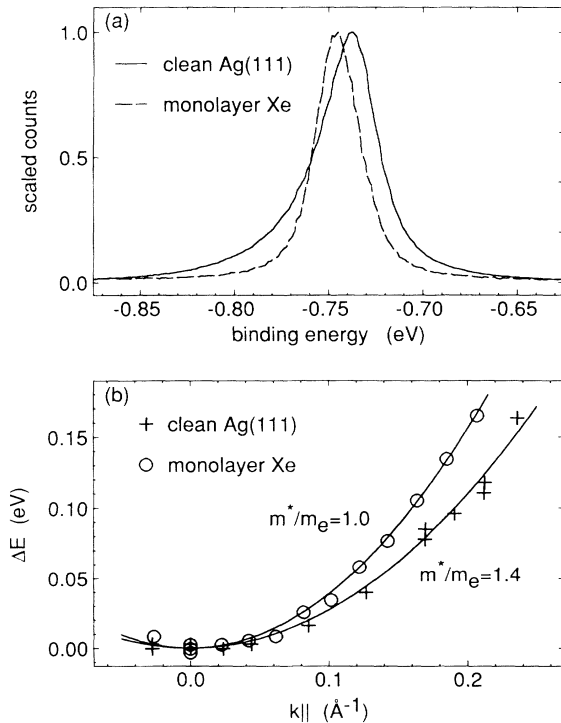

FIG. 2. The $n=1$ image-potential state on clean and monolayer-Xe-covered Ag(111). Two-photon photoemission spectra are shown in (a), and dispersions and effective masses in (b).

dielectric screening would decrease the image potential. If the electron were excluded from the layer, and thereby forced away from the metal, the image force would also decrease. Evidently the monolayer itself exerts an attraction sufficient to offset any such effect. Preliminary calculations suggest that both the polarization of the adsorbate and the electron affinity of the layer should be considered.

Dispersion of the photoelectron energy with momentum along the surface, $E(k_\parallel)$, was measured by varying the polar angle (θ) of the sample surface with respect to the detector. Parallel momentum is $k_\parallel = \hbar^{-1}(2m_e E)^{1/2} \times \sin(\theta)$. To avoid complications arising from dispersion of the initial state, electrons were excited from the continuum of occupied bulk bands, where the density of states is fairly smooth [5]. Along the $\bar{\Gamma}$-$\bar{K}$ azimuth of the clean metal, the $n=1$ dispersion was well fitted by a parabola with an effective-mass ratio $m^*/m_e = 1.3 \pm 0.1$, where m_e is the mass of the electron. This agrees with previous measurements [9,10]. Adsorption of a Xe monolayer produced a marked change in image state dispersion. Dispersion curves for the $n=1$ state on both the clean and Xe-covered surface are shown in Fig. 2(b). For monolayer Xe the image state's effective mass dropped to $(1.0 \pm 0.05)m_e$—for motion parallel to the surface it is effectively a free electron.

For the bare metal surfaces, the characteristics of the image-potential states have been well predicted by the "multiple reflection theory" [3,5,9,11]. Image state binding energies and dispersions depend on the electron's interaction with the band structure of the metal. If on the adsorbate-covered surface the wave function of the electron penetrates to the metal, the band structure will continue to influence the image state. We examined the results of this model given only the work-function change on adsorption, which alters the position of the vacuum level within the projected band gap. Lowering the vacuum level of Ag(111) by 0.45 eV is calculated to decrease the $n=1$ binding energy by 0.1 eV, contrary to the experimental results. There is also a change in dispersion due to the work-function change: m^*/m_e drops from 1.33 to 1.18, as approximated by the method of Giesen et al. [9]. We see that the work-function shift alone is not sufficient to account for the measured value of 1.0 ± 0.05 for the Xe-covered surface. The data are consistent with the simple picture of a 2D free electron bound at the Xe surface, with no influence from the band structure of the metal. We interpret this as screening by the Xe which reduces the penetration of the electron's wave function to the metal surface.

Image states also persisted on a silver surface covered by alkanes. Monolayer coverages of n-hexane produced little or no change in binding energy while cyclohexane caused a decrease of less than 0.1 eV. The dispersion of the $n=1$ state on annealed monolayers was again free-electron-like with $m^*/m_e = 1.0$.

For multilayers the results were remarkable. Successive doses of cyclohexane produced the series of photoelectron spectra shown in Fig. 3. With increasing dose a progression of peaks occurred which can be interpreted as successive reductions in the binding energy of the image state. For a given dose there was a set of peaks which suggest areas of the surface with adsorbate thicknesses differing by discrete molecular layers. The peak distribution shifts as the coverage increases; at least five steps are distinguishable. Between the first and second peaks the binding energy was reduced by 0.06 eV; successive shifts were smaller, converging to a total reduction in binding energy of about 0.2 eV. Hexane, n-heptane, and n-octane gave results similar to cyclohexane. Higher quantum states of the image potential can easily be observed in these spectra. The inset in Fig. 3 expands the region near the vacuum level for an approximately bilayer dose. The $n=2$ and $n=3$ states are not affected by the first few adsorbate layers. A slight shoulder on the $n=2$ peak begins to appear only after more than three layers. As was indicated in Fig. 1, the average distance of the image state electron from the surface increases rapidly for higher members of the Rydberg series. Thus we see variations in the interaction of the electron with the adsorbed layer on the scale of several angstroms.

The multiple peaks at each dose give evidence of incomplete layer growth. Upon annealing, the monolayer or bilayer spectra reduced to single peaks. While the presence of multiple peaks reflects the adsorbate structure, their positions correspond to the layer-by-layer change in electrostatic potential. These spectra provide information on both adsorbate growth morphology and evolution of a thin film toward bulk dielectric properties.

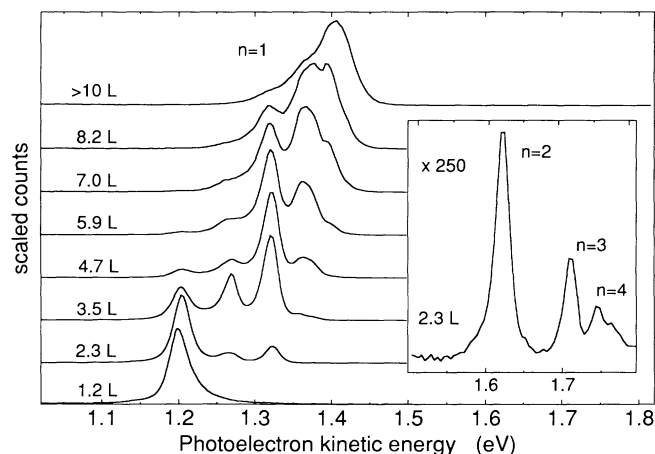Current theory is not adequate to completely interpret these results. We have explored some models based on classical electrostatics for continuous media, but they cannot be expected to apply to monolayers. A central question is how far the electron penetrates into the adsorbate layer. Our preliminary calculations indicate that, in addition to the dielectric constant and film thickness, the electron affinity or the position of the conduction band of the adsorbate is important in determining where the electron will be found. Calculations have been published for image states on dielectric films on metals, but they have also been based on classical electrostatic potentials and are limited to the case where the electron is excluded from the adsorbate layer [12,13]. More appropriate models, suitable to molecular length scales and including adsorbate band structure, have yet to be developed.

A nondispersive peak—its energy did not change with the angle of photoemission—appeared weakly in alkane monolayers and much more strongly in the bilayers. We believe that this feature signals the onset of localization of the bound electron, probably induced by disorder. Angle-resolved spectra of bilayer n-heptane are shown in Fig. 4. It is clear from the data that this technique is well suited to study electron localization as a function of film thickness and composition.

Several other molecules have been examined. The image state persisted, weakly, for thiols and chemisorbed S on Ag(111). For several adsorbates distinct image state peaks were not observed. Adsorption of water, benzene, or perfluorocyclohexane (C_6F_{12}) sharply decreased photoemission from the image state. The survival or extinction of the image state in the presence of various adsorbates is not yet understood and is likely to depend on both the electronic properties and the morphology of the adlayer [14].
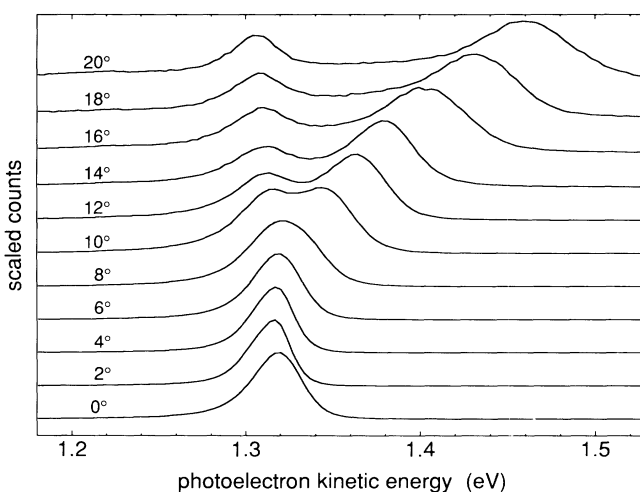

FIG. 3. Spectra of the $n=1$ image state on Ag(111) as a function of cyclohexane dose (1 L$=10^{-6}$ Torrs). The steps correspond closely to the expected number of cyclohexane layers. Inset: The higher Rydberg levels for the 2.3-L dose. Unlike the $n=1$ state, they are unperturbed by the first few adsorbed layers.

FIG. 4. Angle-resolved two-photon photoemission of bilayer n-heptane. A nondispersing peak with energy slightly less than the $n=1$ state emerges at higher angles. The large effective mass is evidence of electron localization by the adsorbed film.

These results demonstrate that two-photon photoemission is a sensitive and general probe of electrons at surfaces and interfaces. Precise measurements of adsorbate-induced changes in the behavior of image states provide a microscopic view of the interaction of electrons with atomically thin films of insulators and the electrostatics of the metal/dielectric/vacuum interface. We believe this technique can be extended to examine a number of important problems: the localization of excess electrons in insulators, metal-nonmetal transitions, magnetic films, and the behavior of electrons at Schottky barriers. Finally, we expect that two-photon photoemission with femtosecond time resolution will develop into a versatile approach to the dynamics of electrons at interfaces and in thin films.

[1] M. W. Cole and M. H. Cohen, Phys. Rev. Lett. 23, 1238 (1969).

[2] P. D. Johnson and N. V. Smith, Phys. Rev. B 27, 2527 (1983).

[3] P. M. Echenique and J. B. Pendry, Prog. Surf. Sci. 32, 111 (1990).

[4] V. Dose, Surf. Sci. Rep. 5, 337 (1985).

[5] W. Steinmann, Appl. Phys. A 49, 365 (1989).

[6] J. Bokor, Science 246, 1130 (1989).

[7] J. Unguris, L. W. Bruch, E. R. Moog, and M. B. Webb, Surf. Sci. 87, 415 (1979).

[8] K. Horn, K. H. Franck, J. A. Wilder, and B. Reihl, Phys. Rev. Lett. 57, 1064 (1986); B. Reihl, in Metallisation and Metal-Semiconductor Interfaces, edited by I. P. Batra, NATO ASI Ser. B, Vol. 195 (Plenum, New York, 1989), p. 397.

[9] K. Giesen, F. Hage, F. J. Himpsel, H. J. Riess, W. Steinmann, and N. V. Smith, Phys. Rev. B 35, 971 (1987).

[10] W. Altmann, V. Dose, and A. Goldman, Z. Phys. B 65, 171 (1986).

[11] N. V. Smith, Phys. Rev. B 32, 3549 (1985).

[12] M. W. Cole, Phys. Rev. B 3, 4418 (1971).

[13] B. Trninić-Radja, M. Šunjić, and Z. Lenac, Phys. Rev. B 40, 9600 (1989); B. Trninić-Radja and M. Šunjić, Phys. Rev. B 42, 7409 (1990).

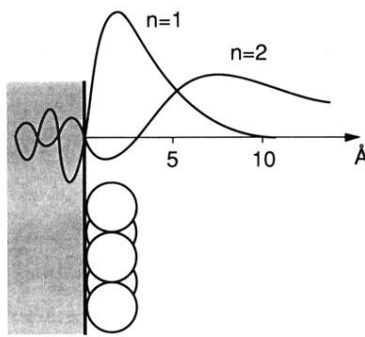[14] M. Donath and K. Ertl, Surf. Sci. Lett. 262, L49 (1992).

FIG. 1. Approximate wave functions for the first two image-potential states of a clean metal surface compared to the thickness of a xenon monolayer.